Vickers, L. P., Compton, J. G., Wall, K. A., Flatgaard, J. E., & Schachman, H. K. (1984) *J. Biol. Chem. 259*, 11027–11035.
Wedler, F. C., & Gasser, F. J. (1974) *Arch. Biochem. Biophys. 163*, 57–68.
Werner, W. E., & Schachman, H. K. (1989) *J. Mol. Biol. 206*, 221–230.
Wyman, J. (1964) *Adv. Protein Chem. 19*, 223–286.
Yang, Y. R., & Schachman, H. K. (1980) *Proc. Natl. Acad. Sci. U.S.A. 77*, 5187–5191.
Yang, Y. R., & Schachman, H. K. (1987) *Anal. Biochem. 163*, 188–195.

Regulation of the Oxidative Phosphorylation Rate in the Intact Cell†

Arthur H. L. From,*,‡ Stevan D. Zimmer,‡ Steve P. Michurski,§ Parakket Mohanakrishnan,§ Valerie K. Ulstad,‡ William J. Thoma,§,∥ and Kâmil Uğurbil*,§

Cardiology Section, Department of Medicine, Minneapolis Department of Veterans Affairs Medical Center and University of Minnesota, One Veterans Drive, Minneapolis, Minnesota 55417, and Departments of Biochemistry and Radiology and Gray Freshwater Biological Institute, University of Minnesota, Navarre, Minnesota 55392

Received November 10, 1988; Revised Manuscript Received August 16, 1989

ABSTRACT: The mechanisms that underlie the balance between the consumption and oxidative generation of ATP in the intact cell are not well-defined. Cytosolic inorganic phosphate (P_i) and ADP levels, the cytosolic ATP/ADP ratio, and the cytosolic phosphorylation potential (PP) have all been proposed as major regulatory variables, the latter as a component of a "near-equilibrium" thermodynamic regulatory scheme. Therefore, the potential regulatory roles of these variables in the intact cell were evaluated with ^{31}P NMR and Langendorff perfused rat hearts; in this preparation, the tissue oxygen consumption rate (MVO_2) can be varied over a wide range. When the exogenous carbon source was varied, none of the proposed regulatory parameters, i.e., the ATP/ADP ratio, PP, or cytosolic ADP level, were found to be uniquely related to MVO_2. Rather, ADP levels at a given MVO_2 decreased progressively for the exogenous carbon sources in the following order: glucose, glucose + insulin, palmitate + glucose, lactate, pyruvate + glucose, and octanoate + glucose. In the octanoate and pyruvate groups, MVO_2^{-1} was linearly dependent upon $[ADP]^{-1}$ with apparent K_m values being in the range previously observed in isolated mitochondria. A similar trend was observed in the MVO_2–$[P_i]$ relationship. The present findings suggest that exogenous carbon sources which effectuate deregulation of intramitochondrial NADH generation lower cytosolic ADP and P_i to levels which are limiting to the rate of oxidative phosphorylation. For other carbon sources, the processes controlling the rate of NADH generation also participate in determining the rate of oxidative ATP synthesis. However, this control must be exerted kinetically rather than through a near-equilibrium thermodynamic mechanism as indicated by the present data and prior kinetic studies of the ATP synthetic process in both isolated mitochondria and intact myocardium [La Noue, K. F., et al. (1986) *Biochemistry 25*, 7667–7675; Kingsley-Hickman, P., et al. (1987) *Biochemistry 26*, 7501–7510].

It is well-known that, in the intact cell, the rate of ATP production is tightly coupled to the rate of ATP consumption. In cell types that rely primarily on oxidative metabolism, this tight coupling implies that the rate of oxygen consumption by mitochondria is highly regulated by cytoplasmic processes. However, the biochemical signals that mediate this regulation and that relate the rates of ATP synthesis and utilization are unclear. Studies of isolated mitochondrial preparations have led to hypotheses that phosphate donor/acceptor status (i.e., ADP and/or P_i),[1] the ATP/ADP ratio, or phosphorylation potential (defined as $[ATP]/[P_i][ADP]$) may be regulatory (e.g., Chance and Williams (1955), Erecinska and Wilson (1982), and Tager et al. (1983)]. However, studies with isolated mitochondria are limited in that many of the parameters that may influence respiratory regulation, such as the carbon source required for TCA cycle operation and NADH generation, may be set by the experimenter to conditions that do not necessarily apply to the intact cell. Therefore, in such studies it is difficult to fully evaluate all potential regulatory influences associated with mitochondrial NADH[2] synthesis that may be of great significance in intact tissues.

In this paper, we present detailed studies of the mechanisms of respiratory regulation conducted with ^{31}P NMR spectroscopy and intact perfused hearts. The myocardium was the

† Funding provided by NIH Grants RO1 HL33600, HL32427, IKO4 HL01241, and KI11 HL02014 and by AHA-MN Affiliate and Department of Veterans Affairs Medical Research Funds.

* Correspondence and reprint requests should be addressed to these authors.
‡ Department of Veterans Affairs Medical Center and University of Minnesota.
§ University of Minnesota.
∥ Present address: Department of Radiology, University of Iowa, Iowa City, IA 52242.

[1] Abbreviations: MVO_2, myocardial oxygen consumption rate; LV, left ventricle; EDP, left ventricular end diastolic pressure; RPP, rate pressure product; PP, phosphorylation potential; PDH, pyruvate dehydrogenase; TCA, tricarboxylic acid; P_i, inorganic phosphate; G, glucose; I, insulin; PG, pyruvate + glucose; Palm, palmitate + glucose; Oct, octanoate + glucose; Lac, lactate; NMR, nuclear magnetic resonance; gdw, gram dry weight.

[2] Unless specifically stated otherwise, NAD and NADH refer to mitochondrial contents; ATP, ADP, and P_i refer to cytosolic contents.

0006-2960/90/0429-3731$02.50/0

tissue of choice because the myocardial oxygen consumption rate could be varied over a large range by simply manipulating mechanical output. ^{31}P NMR spectroscopy affords the ability to measure the content of the phosphorylated metabolites in the intact cell nondestructively, thereby avoiding the limitations encountered in procedures based on cell extraction methods.

Recently, we (From et al., 1986; Robitaille et al., 1990) and others (Balaban et al., 1986) have presented data derived from ^{31}P NMR studies that examine respiratory regulation in the intact myocardium. In a preliminary report of our studies with perfused rat hearts (From et al., 1986), we found that myocardial mechanical output and MVO_2 were related to myocardial ADP levels by Michaelis–Menten kinetics (single-substrate kinetic model) when pyruvate was used as the exogenous carbon source and MVO_2 was altered by manipulation of heart rate and by exposure to an inotropic agent. However, there was no such relationship when glucose ± insulin was the only carbon source in the perfusate. In recent studies (Balaban et al., 1986; Robitaille et al., 1990) carried out with in situ canine myocardium, myocardial creatine phosphate (CP), pH, and ATP (and, therefore, estimated ADP levels) did not change in relation to increasing mechanical output; these observations indicated that, under in vivo conditions, changes in [ADP] could not account for work-associated changes in the rate of oxidative phosphorylation.

The current ^{31}P NMR investigation extends our preliminary observations by examining the relationship between phosphate donor/acceptor status and oxygen consumption under additional carbon source conditions and by evaluating the effects of inhibition of endogenous lipid consumption and PDH deregulation upon these variables. Taken together with recent data on the kinetics of H^+-ATPase in the intact heart (Kingsley-Hickman et al., 1987) and in isolated mitochondria (La Noue et al., 1986), which are incompatible with the "near-equilibrium" hypothesis (Erecinska & Wilson, 1982), the present observations strongly suggest that, in the presence of abundant O_2, the rate of oxidative phosphorylation is kinetically regulated by the availability of its substrates, NADH, ADP, and P_i. Coupling between mechanical work and MVO_2 and the role of Ca^{2+} ion and carbon substrate delivery to the TCA cycle are discussed within the context of this model of respiratory regulation and give further support to the concept that regulation of metabolic events occurring proximal to the H^+-ATPase plays a major role in the control of oxidative phosphorylation in the intact myocardium.

Materials and Methods

Langendorff Perfusion. In this study, hearts were removed from pentobarbitol-anesthetized and mechanically ventilated Sprague-Dawley (400–500 g) rats, rapidly chilled, and placed on the perfusion system, which has recently been described in detail (Ugurbil et al., 1986). Briefly, an isovolumic Langendorff perfusion technique was employed; perfusion pressure was 90 mmHg. The physiologic buffer contained 119 mM NaCl, 28 mM $NaHCO_3$, 1.2 mM $MgCl_2$, 4.7 mM KCl, 1.2 mM KH_2PO_4, 1.8 mM $CaCl_2$, and 0.1 mM EDTA. The added carbon sources included 15 mM glucose ± 20 IU of regular insulin/L (G and GI), 10 mM sodium pyruvate + 10 mM glucose (PG), 10 mM sodium lactate (Lac), and palmitate adsorbed to bovine serum albumin + 10 mM glucose [Palm; prepared as described by Pearce et al. (1979)]; for the last carbon source condition, the final perfusate albumin and palmitate contents were approximately 0.5 g % and 0.5 mM, respectively. Additional groups of hearts were studied with 1 and 2 mM octanoate + 10 mM glucose (Oct) perfusate; albumin concentrations were 0.5 and 1 g %, respectively.

Table I: Workstate Protocol[a]

I	HR = 180 beats/min; LVEDP = 8 mmHg
II	HR = 300 beats/min; LVEDP = 8 mmHg
III	HR = 300 beats/min; LVEDP = 8 mmHg; [dobutamine] = 40 ng/mL of perfusate
IV	HR = 450 beats/min; LVEDP = 17 mmHg; [dobutamine] = 40 ng/mL of perfusate
V	HR = 450 beats/min; LVEDP = 17 mmHg; [dobutamine] = 80 ng/mL of perfusate
VI	HR = 600 beats/min; LVEDP = 17 mmHg; [dobutamine] = 80 ng/mL of perfusate

[a] HR = heart rate; LVEDP = left ventricular end diastolic pressure.

When the Na salt of pyruvate or lactate was added, perfusate NaCl was correspondingly lowered.

In experiments where lipid metabolism was blocked, 13 μM 4-bromocrotonic acid (BCA) was added to the perfusate (Hutter et al., 1984). In additional experiments, 1 mM dichloroacetic acid (DCLA) was added to the perfusate to activate PDH (Dennis et al., 1979).

The perfusion system was designed to permit measurement of left ventricular pressure (via an intraventricular balloon) and MVO_2 (via a Clark electrode placed in the perfusate effluent stream). Heart rate was controlled by pacing after the atrio–ventricular mode was crushed. Cardiac mechanical output (quantitated as the product of left ventricular peak systolic pressure and heart rate; RPP) was altered by means of variations in (paced) heart rate, left ventricular filling volume (via the intraventricular balloon), and infusion of dobutamine. The workstate protocol utilized is shown in Table I. All data were obtained during 10-min sampling periods, which were begun following stabilization of function (usually 3–10 min) after change of workstate.

^{31}P NMR Measurements. The NMR techniques utilized have been described in detail (Ugurbil et al., 1986). Briefly, ^{31}P NMR measurements (obtained in a Nicollet 360 wide-bore spectrometer) were conducted at 146.1 MHz with a single-turn solenoidal probe of our design and manufacture. The myocardial ATP and CP contents were obtained from fully relaxed NMR spectra and a reference signal. ADP content was calculated from the creatine kinase equilibrium relationship (Lawson & Veech, 1979; $[ATP][Cr]/[ADP][H^+][CP] = 1.66 \times 10^9\ M^{-1}$). A myocardial creatine (Cr) plus creatine phosphate (CP) content of 68.5 ± 6.6 μmol gdw^{-1} (Williamson, 1966) was used in all ADP calculations. The cytosolic pH value was measured from the P_i chemical shift. Under all workstate and carbon source conditions examined, the cytosolic pH was constant in a given heart and ranged between 7.0 and 7.1. Therefore, in all ADP calculations, a cytosolic pH value of 7.05 was used. The cytosolic pH values observed in the present investigation are comparable to those previously reported (Bailey et al., 1981).

To obtain accurate measurements for cytosolic P_i, P_i content was measured at one workload in hearts perfused with P_i-free media under otherwise identical conditions for several of the substrates (n = 5 for each group). P_i contents at other workloads were obtained from these data and the change in P_i content that was measured by difference spectra. Most metabolite measurements were expressed as content (e.g., nanomoles or micromoles gdw^{-1}). Cytosolic concentrations were estimated with a cytosolic volume of 0.44 mL (g wet wt)$^{-1}$ (Morgan et al., 1964) and a measured wet to dry weight ratio for each heart. This ratio averaged 5.7 ± 0.1 under our experimental conditions.

Data Analysis. The data are expressed as mean ± the standard error of the mean in all tables and figures. The kinetic analyses were performed in two ways. In the first, the

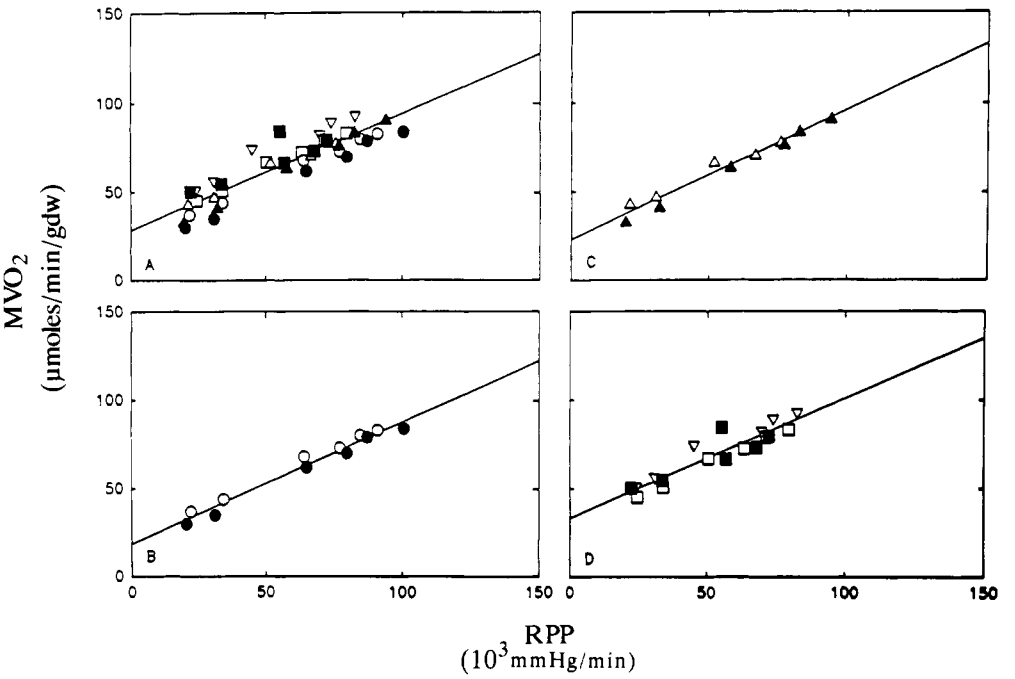

FIGURE 1: General relationship between RPP and MVO_2 for different substrates. Panel A shows the results for all substrates. Data for subgroups of related substrates are shown in subsequent panels: (panel B) G and GI; (panel C) Lac and PG; (panel D) Palm, Oct-1, and Oct-2. Symbols: (Open circles) G; (closed circles) GI; (open upright triangles) PG; (closed upright triangles) Lac; (open squares) Oct-1; (closed squares) Oct-2; (inverted open triangles) Palm. The abbreviations are as defined in the text for this and other legends; for the Oct group, 1 and 2 refer to perfusate concentration of octanoate in millimolar.

relationship between ADP or P_i content and MVO_2 was evaluated with Lineweaver–Burk plots by linear regression analysis and a single-substrate Michaelis–Menten model. In the second, kinetic data relating MVO_2 to ADP and P_i contents were fitted to a two-substrate Michaelis–Menten kinetic model with the nonlinear optimization algorithm of Nelder and Mead (1965) in order to obtain either four parameters, K_m^a, K_m^p, K_i^a, and V_{max} (see eq 1 under Results for definitions), or three parameters, K_m^a, K_m^p, and V_{max}, after K_i^a was fixed at 1.4 μM, which corresponds to a previously reported measurement in isolated mitochondria (Stoner & Sirak, 1979). In this optimization, χ^2 was minimized; χ^2 is defined as the sum of (calculated MVO_2 − measured $MVO_2)^2/\sigma$ for all data points divided by the number of data points, and σ is the experimental error in MVO_2. "Covariance" among the parameters was examined by fixing K_i^a at 1.4 μM and calculating χ^2 in three-dimensional parameter space defined by (K_m^a, K_m^p, V_{max}), and delineating the boundries of the volume in this parameter space within which χ^2 was equal to or less than minimum χ^2 plus 1. K_i^a was fixed because the fits were in general very insensitive to changes in this parameter.

Drugs and Reagents. The 4-bromocrotonic acid was synthesized according to a published method (Bradshaw et al., 1969). All other drugs and reagents used were of the purest grade available from commercial sources.

Results

Effects of Exogenous Carbon Source Type upon Mechanical Performance and High-Energy Phosphate Compound Contents

Myocardial Performance in Relation to Carbon Source. The general relationship between myocardial mechanical output measured as RPP and MVO_2 for all major carbon source conditions is shown in Figure 1. There is a linear relationship between RPP and MVO_2 for all carbon source groups over the range studied, and the relationship is comparable for all groups but palmitate and octanoate. For these groups, MVO_2 was elevated at a given RPP relative to other carbon sources, and while the slope of the MVO_2–RPP relationship was comparable to those of the remaining groups, the intercept was different. The modest elevation of MVO_2 in relation to RPP in the fatty acid groups may relate to the obligatory increase in oxygen consumption required to maintain a given level of ATP synthesis when a change from carbohydrate to lipid utilization was made (Pearce et al., 1979) as well as to oxygen "wastage" of several possible etiologies (Mjos, 1971). The primary point demonstrated by the MVO_2–RPP data is that the ranges of MVO_2 and RPP are not constrained by the particular exogenous carbon source chosen or, put another way, that *no* carbon source was limiting to metabolic or mechanical function.

High-Energy Phosphate Compound Levels in Relation to Carbon Source. Tables II–V list the ATP, CP, P_i, and calculated ADP contents at different workstates under all carbon source conditions. Representative spectra that were used to obtain these data are illustrated in Figures 2 and 3. Figure 2 displays typical spectra recorded at different workstates for a PG-perfused heart. The increase in cytosolic P_i content at the workstates associated with high RPP and MVO_2 values is easily noted. Figure 3 shows similar data obtained under identical workstates from a glucose-perfused heart. Comparison between Figures 2 and 3 illustrates that, despite approximately the same MVO_2 and RPP achieved by these hearts for the same workstate, the CP and P_i contents were significantly different.

In all groups (Tables II–IV), ATP content fell modestly over the range of MVO_2 values achieved. CP content was relatively stable in the GI group, fell and then partially recovered with increasing MVO_2 in the G group, and fell monotonically with increasing MVO_2 in the PG, Palm, and Lac groups.

As can be calculated from the data in Tables II–IV, the CP/ATP ratios at the highest MVO_2 values exceeded those observed at the lowest MVO_2 values in the G, GI, and Palm groups. Further, a tendency for the CP/ATP ratio to decrease as MVO_2 increased from workstate I to workstate III was

Table II: ATP, CP, ADP, and P_i Contents and RPP and MVO_2 in Glucose ± Insulin Perfused Hearts at Six Workstates[a]

	I	II	III	IV	V	VI
ATP (μmol gdw^{-1})						
G	25.3 ± 1.4	24.4 ± 1.6	23.0 ± 1.2	22.7 ± 1.1	21.5 ± 1.2	20.3 ± 1.1
GI	23.2 ± 2.0	22.9 ± 2.0	22.0 ± 1.6	21.7 ± 1.4	21.8 ± 1.3	20.6 ± 1.3
CP (μmol gdw^{-1})						
G	37.5 ± 3.3	31.7 ± 2.4	26.9 ± 1.6	32.5 ± 1.8	34.0 ± 2.0	35.4 ± 2.5
GI	43.1 ± 2.8	41.9 ± 2.9	40.9 ± 1.7	43.5 ± 2.4	43.0 ± 3.0	41.7 ± 2.9
ADP (nmol gdw^{-1})						
G	139 ± 17.9	190 ± 25.8	244 ± 27.3	167 ± 18.7	147 ± 10.4	130 ± 14.9
GI	94 ± 12.9	100 ± 15.2	109 ± 15.2	90 ± 10.1	93 ± 10.4	91 ± 10.4
P_i (μmol gdw^{-1})						
G	99.9 ± 1.6	12.9 ± 1.6	18.2 ± 3.2	20.6 ± 3.2	20.5 ± 3.6	24.1 ± 4.2
GI	5.3 ± 1.0	5.7 ± 1.1	8.6 ± 4.7	10.2 ± 2.6	14.5 ± 4.6	17.7 ± 4.8
RPP (10^3 × mmHg/min)						
G	22.0 ± 1.3	34.3 ± 2.1	64.0 ± 6.2	77.2 ± 4.6	84.8 ± 4.6	91.2 ± 5.8
GI	20.6 ± 2.0	31.2 ± 2.1	65.0 ± 8.1	79.9 ± 6.1	87.4 ± 6.2	100.7 ± 5.6
MVO_2 (μmol min^{-1} gdw^{-1})						
G	37.2 ± 1.5	43.9 ± 1.3	68.3 ± 2.6	73.0 ± 2.9	80.1 ± 2.9	82.7 ± 3.4
GI	30.1 ± 2.1	34.6 ± 2.7	61.5 ± 5.2	69.5 ± 4.6	78.5 ± 4.2	83.8 ± 3.9

[a] Workstates as defined in Table I; G = 15 mM glucose perfusate (n = 8); GI = 15 mM glucose + 20 IU of insulin/L (n = 6); values are mean ± SE. Errors for ADP were calculated from the standard errors of CP/ATP ratio, ATP, and total creatine (68.6 ± 6.6) using the equation [(fractional error (FE) in ADP)^2 = (FE ATP)^2 + (FE total creatine)^2 + (FE CP/ATP)^2].

Table III: ATP, CP, ADP, and P_i Contents and RPP and MVO_2 in Pyruvate + Glucose Perfused and Lactate-Perfused Hearts at Six Workstates[a]

	I	II	III	IV	V	VI
ATP (μmol gdw^{-1})						
PG	27.1 ± 1.6	27.4 ± 1.5	25.6 ± 1.5	25.2 ± 1.2	24.4 ± 1.1	22.5 ± 1.1
Lac	27.5 ± 1.4	27.3 ± 0.5	26.8 ± 0.7	25.2 ± 0.8	25.6 ± 1.1	23.4 ± 0.9
CP (μmol gdw^{-1})						
PG	60.2 ± 3.7	58.8 ± 3.4	50.5 ± 2.8	50.4 ± 2.4	50.3 ± 2.5	47.0 ± 2.2
Lac	58.1 ± 2.1	54.5 ± 1.7	50.1 ± 1.8	52.1 ± 2.1	51.6 ± 2.2	49.3 ± 2.2
ADP (nmol gdw^{-1})						
PG	25 ± 2.4	31 ± 3.6	61 ± 7.2	61 ± 6.9	59 ± 6.8	69 ± 7.7
Lac	33 ± 3.5	47 ± 4.8	66 ± 6.9	54 ± 5.6	54 ± 5.8	61 ± 6.6
P_i (μmol gdw^{-1})						
PG	0.9 ± 0.5	1.8 ± 0.2	2.6 ± 0.8	5.4 ± 1.1	7.4 ± 1.4	10.0 ± 1.5
Lac						
RPP (10^3 × mmHg/min)						
PG	21.6 ± 0.8	31.2 ± 1.4	52.0 ± 3.2	66.7 ± 3.2	75.8 ± 3.2	82.6 ± 3.8
Lac	30.7 ± 1.1	34.3 ± 1.8	58.9 ± 2.8	76.7 ± 2.8	82.2 ± 3.0	92.8 ± 2.7
MVO_2 (μmol min^{-1} gdw^{-1})						
PG	43.5 ± 2.7	47.5 ± 2.3	67.0 ± 2.5	71.1 ± 2.1	78.2 ± 2.4	84.0 ± 2.5
Lac	33.9 ± 1.5	41.4 ± 0.8	84.2 ± 2.2	74.8 ± 2.3	81.6 ± 2.1	87.9 ± 2.2

[a] PG = 10 mM pyruvate + 10 mM glucose perfusate (n = 12); Lac = 10 mM lactate perfusate (n = 10). See Table II footnote *a* for error analysis.

Table IV: ATP, CP, ADP, and P_i Contents and RPP and MVO_2 in Palmitate + Glucose and Octanoate + Glucose Perfused Hearts at Six Workstates[a]

	I	II	III	IV	V	VI
ATP (μmol gdw^{-1})						
Palm	24.4 ± 0.9	24.2 ± 1.0	23.6 ± 0.8	22.9 ± 1.0	21.0 ± 0.9	19.8 ± 0.9
Oct-2	25.9 ± 1.4	24.6 ± 1.0	24.5 ± 1.2	22.3 ± 1.3	20.2 ± 1.2	19.6 ± 1.1
CP (μmol gdw^{-1})						
Palm	48.3 ± 2.3	47.5 ± 2.6	47.0 ± 2.3	46.7 ± 2.4	45.4 ± 2.3	43.0 ± 2.4
Oct-2	60.3 ± 1.9	57.3 ± 2.6	52.4 ± 3.0	49.0 ± 3.1	47.0 ± 2.7	43.0 ± 2.6
ADP (nmol gdw^{-1})						
Palm	69 ± 7.4	72 ± 7.4	73 ± 7.8	72 ± 8.1	75 ± 7.8	79 ± 8.8
Oct-2	23 ± 2.7	32 ± 3.5	51 ± 6.0	59 ± 7.3	62 ± 7.5	74 ± 8.5
P_i (μmol gdw^{-1})						
Palm	3.0 ± 0.6	3.0 ± 0.6	7.8 ± 2.0	11.0 ± 2.6	14.8 ± 3.1	19.7 ± 3.7
Oct-2						
RPP (10^3 × mmHg/min)						
Palm	24.5 ± 0.9	31.2 ± 1.7	45.4 ± 2.2	70.1 ± 2.8	74.1 ± 2.7	82.8 ± 2.8
Oct-2	25.6 ± 1.3	36.6 ± 1.1	54.9 ± 1.6	65.7 ± 1.9	71.3 ± 2.2	82.2 ± 2.4
MVO_2 (μmol min^{-1} gdw^{-1})						
Palm	50.3 ± 2.5	55.6 ± 2.5	73.8 ± 2.5	81.8 ± 2.9	88.7 ± 3.1	92.2 ± 2.9
Oct-2	51.1 ± 1.3	55.5 ± 1.2	68.6 ± 1.1	73.7 ± 1.5	79.4 ± 1.2	84.0 ± 1.4

[a] Palm = 0.5 mM palmitate + 10 mM glucose perfusate (n = 14); Oct-2 = 2 mM octanoate + 10 mM glucose perfusate (n = 10). See Table II footnote *a* for error analysis.

noted in the G, GI, and Lac groups. The reversal of this fall of the CP/ATP ratio (beginning with workstate IV) was most marked in the G group and was temporally correlated with the onset of metabolic dependence upon endogenous lipid

Table V: Effects of BCA on Glucose- and Lactate-Perfused Hearts and Effects of DCLA after BCA in Glucose-Perfused Hearts[a]

	I	II	III	IV	V	VI
ATP (μmol gdw^{-1})						
G + BCA	32.5 ± 2.1	31.8 ± 2.2	29.0 ± 2.6	26.5 ± 1.6	23.3 ± 2.0	19.3 ± 1.7
G + BCA + DCLA	28.9 ± 1.4	28.6 ± 1.5	27.5 ± 1.8	25.6 ± 1.5	23.0 ± 1.9	18.1 ± 2.4
Lac + BCA	28.4 ± 1.7	28.4 ± 1.8	27.5 ± 1.2	27.3 ± 1.2	26.5 ± 1.3	25.0 ± 1.3
CP (μmol gdw^{-1})						
G + BCA	37.0 ± 1.1	33.6 ± 1.7	31.0 ± 2.2	29.5 ± 1.6	23.3 ± 2.0	15.8 ± 2.3
G + BCA + DCLA	46.0 ± 3.0	43.8 ± 4.6	37.8 ± 2.6	36.5 ± 2.1	29.6 ± 2.5	18.8 ● 2.8
Lac + BCA	60.0 ± 2.2	55.6 ± 2.3	51.5 ± 2.4	50.9 ± 2.7	48.6 ± 2.6	45.0 ± 3.3
ADP (nmol gdw^{-1})						
G + BCA	185 ± 23.2	220 ± 27.5	230 ± 32.4	235 ± 29.7	302 ± 43.1	445 ± 70.1
G + BCA + DCLA	96 ± 12.7	110 ± 14.9	149 ± 20.5	155 ± 18.5	169 ± 22.9	320 ± 60.5
Lac + BCA	27 ± 3.2	44 ± 5.3	62 ± 6.7	64 ± 6.5	73 ± 8.1	88 ± 9.9
RPP (10^3 × mmHg/min)						
G + BCA	27.5 ± 1.9	37.7 ± 1.7	49.4 ± 1.9	51.7 ± 2.2	42.3 ± 3.6	40.4 ± 4.2
G + BCA + DCLA	26.3 ± 1.6	37.7 ± 3.3	58.0 ± 1.2	78.2 ± 3.2	67.9 ± 6.7	60.6 ± 9.1
Lac + BCA	20.1 ± 1.3	31.0 ± 1.9	45.2 ± 2.4	65.9 ± 2.0	76.4 ± 1.6	82.2 ± 1.9
MVO_2 (μmol min^{-1} gdw^{-1})						
G + BCA	40.8 ± 4.7	48.0 ± 5.1	60.0 ± 7.4	59.0 ± 4.9	54.0 ± 5.7	47.0 ± 5.3
G + BCA + DCLA	42 ± 2	48 ± 2	70 ± 2	76 ± 3	73 ± 5	62 ± 5
Lac + BCA	38.6 ± 1.8	44.9 ± 1.9	63.5 ± 2.3	73.0 ± 1.3	81.0 ± 2.0	88.5 ± 2.9

[a] G + BCA = 10 mM glucose + 13 μM 4-bromocrotonic acid perfusate (n = 6); G + BCA + DCLA = 10 mM glucose + 13 μM 4-bromocrotonic acid + 1 mM dichloroacetic acid perfusate (n = 7); Lac + BCA = 10 mM lactate + 13 μM 4-bromocrotonic acid perfusate (n = 6). See Table II footnote *a* for error analysis.

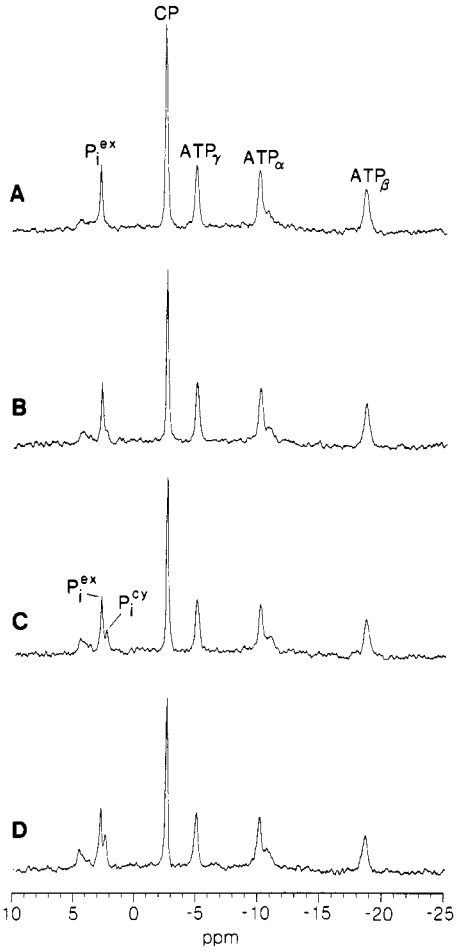

FIGURE 2: Representative spectra recorded from a heart perfused with PG as the exogenous carbon source at four different workstates: workstate I (A), workstate II (B), workstate IV (C), and workstate VI (D). P_i^{ex} = extracellular P_i and P_i^{cy} = intracellular P_i.

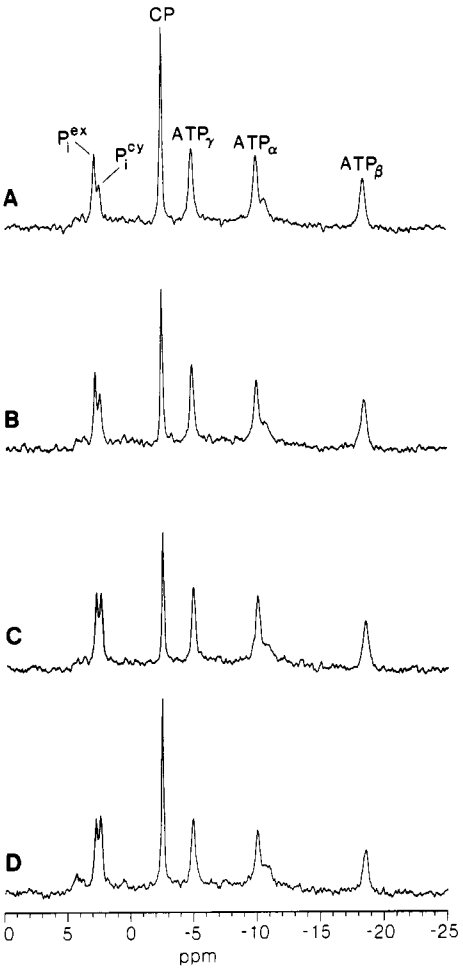

FIGURE 3: Representative spectra recorded from a heart perfused with G as the exogenous carbon source at four different workstates. All experimental parameters are the same as in Figure 2 except for the change in the exogenous carbon source.

consumption as demonstrated by the studies with 4-bromocrotonic acid described below.

Relationship between MVO_2 and ATP/ADP Ratio and PP

MVO_2–ATP/ADP Relationship. The mean ATP/ADP ratios are plotted against MVO_2 in Figure 4A. The ATP/ADP ratio at a given MVO_2 varied considerably in relation to carbon source; indeed, the ranges of the values of the G and GI groups do not overlap those of the other groups. The relationship between the ATP/ADP ratio and MVO_2 also varied substantially between substrates. The ATP/ADP ratio

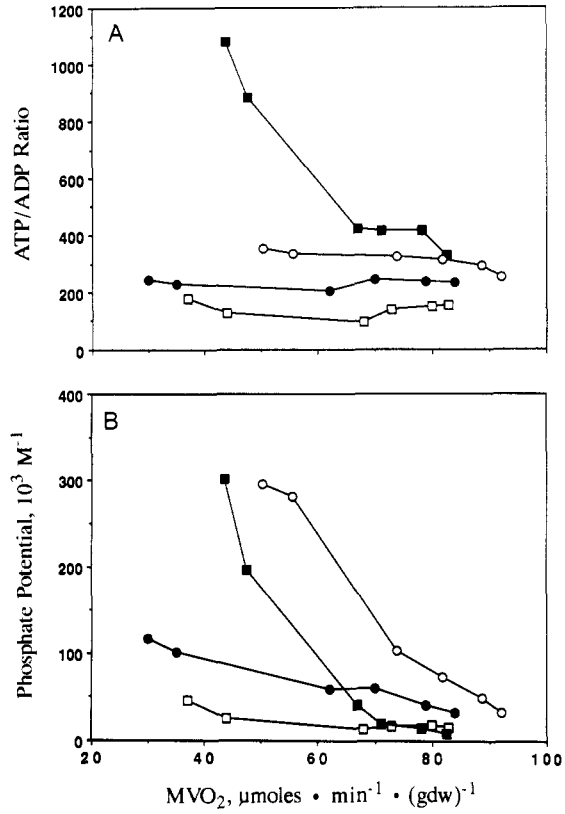

FIGURE 4: The mean ATP/ADP ratio (panel A) and the phosphate potential (PP) (panel B) as a function of MVO_2 for four different exogenous substrates. Symbols: (open squares) G; (closed circles) GI; (closed squares) PG; (open circles) Palm. PP data plotted for PG group are actual values × 10^{-1}.

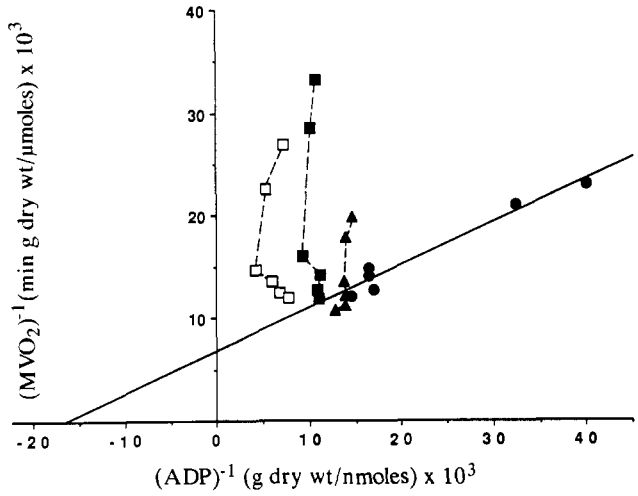

FIGURE 5: MVO_2^{-1} versus $[ADP]^{-1}$ for four different exogenous substrates. Symbols: (open squares) G; (closed squares) GI; (closed circles) PG; (closed triangles) Palm.

fell modestly in the Palm group and showed minimal change in the G and GI groups; in contrast, the ATP/ADP ratio fell sharply with increasing MVO_2 in the PG group. The Oct-2 and Lac groups showed changes similar to that of the PG group (this is not shown in Figure 4A but can be readily verified from perusal of data in Tables III and IV).

MVO_2–PP Relationship. For each exogenous carbon source evaluated, PP fell as MVO_2 increased (Figure 4B; note difference in scale for PG group). However, as in the case of ATP/ADP values, PP values at a given MVO_2 were markedly dependent on carbon source (a consequence of the different cytosolic ADP and P_i contents maintained for each carbon

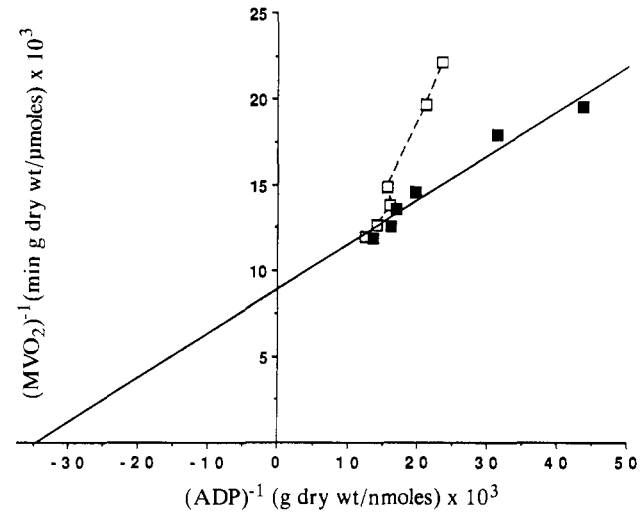

FIGURE 6: MVO_2^{-1} versus $[ADP]^{-1}$ in hearts perfused with Oct-1 (open squares) and Oct-2 (closed squares).

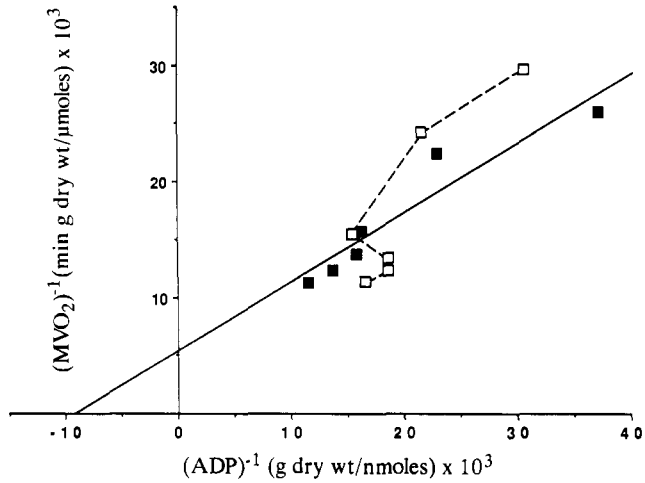

FIGURE 7: MVO_2^{-1} vs $[ADP]^{-1}$ in hearts perfused with Lac (open squares) or Lac + 13 μM BCA (closed squares).

Table VI: Apparent K_m and V_{max} Values Derived from the MVO_2^{-1} vs $[ADP]^{-1}$ Relationship for Three Different Carbon Source Conditions[a]

carbon source	K_m(ADP) (μM)	V_{max} (μmol of O_2 min^{-1} gdw^{-1})	r	p
PG	25 ± 5	148 ± 24	0.98	<0.001
Oct-2	12 ± 1.7	114 ± 78	0.98	<0.001
Lac + BCA	47 ± 21	193 ± 78	0.95	<0.005

[a] Exogenous carbon sources as defined in Tables II–V; r and p refer to linear regression analysis applied to Lineweaver–Burk plot. ADP in micromolar was obtained from ADP in nmol gdw^{-1} by dividing by 2.51. This factor was calculated as described under Materials and Methods.

source at a given workstate); thus, a given MVO_2 was not associated with a unique value of PP when carbon source group comparisons were made.

Kinetic Analyses—Single-Substrate Model

MVO_2–ADP Content Relationship. Figure 5 depicts the relationship between inverse mean ADP content and MVO_2 values for PG, Palm, GI, and G groups. Similar data are presented in Figure 6 for Oct-1 and Oct-2 groups. Finally, Figure 7 illustrates the data for the Lac and Lac + BCA groups. These data (see Tables II–V as well) clearly demonstrate that, for a given MVO_2, ADP levels are substantially different with different exogenous carbon sources and a unique

Table VII: Apparent K_m and V_{max} Values Derived from the MVO_2^{-1} vs $[P_i]^{-1}$ Relationship for Two Different Carbon Source Conditions[a]

carbon source	$K_m(P_i)$ (mM)	V_{max} (μmol of O_2 min^{-1} gdw^{-1})	r	p
PG	0.38 ± 0.08	85 ± 9	0.93	<0.01
Palm	1.3 ± 0.13	105 ± 6	0.99	<0.001

[a] Exogenous carbon sources as defined in Tables II–IV; r and p refer to linear regression analysis applied to Lineweaver–Burk plots. P_i in millimolar was obtained from P_i in μmol gdw^{-1} by dividing by 2.51. This factor was calculated as described under Materials and Methods.

and singular relationship between ADP content and MVO_2 does not exist.

The MVO_2^{-1} vs $[ADP]^{-1}$ data for PG, Oct-2, and Lac + BCA groups are readily fitted to a straight line. *Apparent*[3] K_m and V_{max} values calculated from this linear dependence are given in Table VI. These values fall within the range of values measured with isolated mitochondrial suspensions (Chance & Williams, 1955; Jacobus et al., 1982; LaNoue et al., 1986).[4] It should be noted that, with these exogenous carbon sources, the ADP levels at the workstate with the lowest MVO_2 were significantly lower than the calculated K_m values; with increasing MVO_2, the ADP levels increased to become approximately comparable to or marginally greater than the calculated K_m values.

MVO_2–P_i Content Relationship. The P_i values followed a pattern similar to that of ADP for the different substrates (Table II–IV). The PG and G groups had the lowest and highest P_i values, respectively. For all groups in which it could be evaluated, MVO_2^{-1} vs $[P_i]^{-1}$ interdependence was sufficiently linear to obtain apparent K_m and V_{max} values with a single-substrate Michaelis–Menten kinetic model. Only for the PG and Palm groups (Table VII) were the calculated K_m values within the range obtained with isolated mitochondria (Stoner & Sirak, 1979). P_i values were not determined for Lac and Oct groups.

P_i Content Influence on MVO_2–ADP Content Relationship. In the PG group, both P_i and ADP contents are low and change with MVO_2. In a separate group of hearts this relationship was examined under conditions of elevated P_i content while the exogenous carbon source remained the same. A group of PG-perfused hearts (n = 5) were subjected to an 18-min period of total global ischemia at a cardiac temperature that was less than 37 °C during the ischemic period. The mechanical responses and MVO_2 values for these hearts prior to and following the ischemic insult have been reported previously (Zimmer et al., 1987). This group of hearts had normal postischemic mechanical function and a normal MVO_2/RPP relationship over the same range of workstates utilized for the nonischemic groups described above. Postischemic ATP content in this group was reduced to 58% of control (25.5 ± 1.6 to 14.8 ± 2.3 μmol gdw^{-1}) and was relatively stable over the range of workstates that were achieved. CP levels were normal postischemia (56.6 ± 3.6 μmol gdw^{-1}) and fell modestly with increasing workload. Most importantly, cytosolic P_i contents were dramatically elevated postischemia and attained values roughly comparable to those displayed by the normal G group (increasing from 6.9 ± 1.4 to 22.7 ± 2.9 μmol gdw^{-1}) over the MVO_2 range examined). As shown in Figure 8A, in the postischemic group MVO_2^{-1} was still linearly dependent on $[ADP]^{-1}$ with a calculated apparent K_m for ADP of 14 ± 2 μM, a value only modestly lower than that observed in the control PG group. V_{max} was unaltered at 163 ± 17 μmol gdw^{-1}. While the P_i levels were elevated, they still exhibited a linear MVO_2^{-1} vs $[P_i]^{-1}$ interdependence (Figure 8B), yielding apparent K_m and V_{max} values of 4.5 ± 0.9 mM and 141 ± 15 μmol min^{-1} gdw^{-1}, respectively, when fitted to a single-substrate Michaelis–Menten kinetic model.

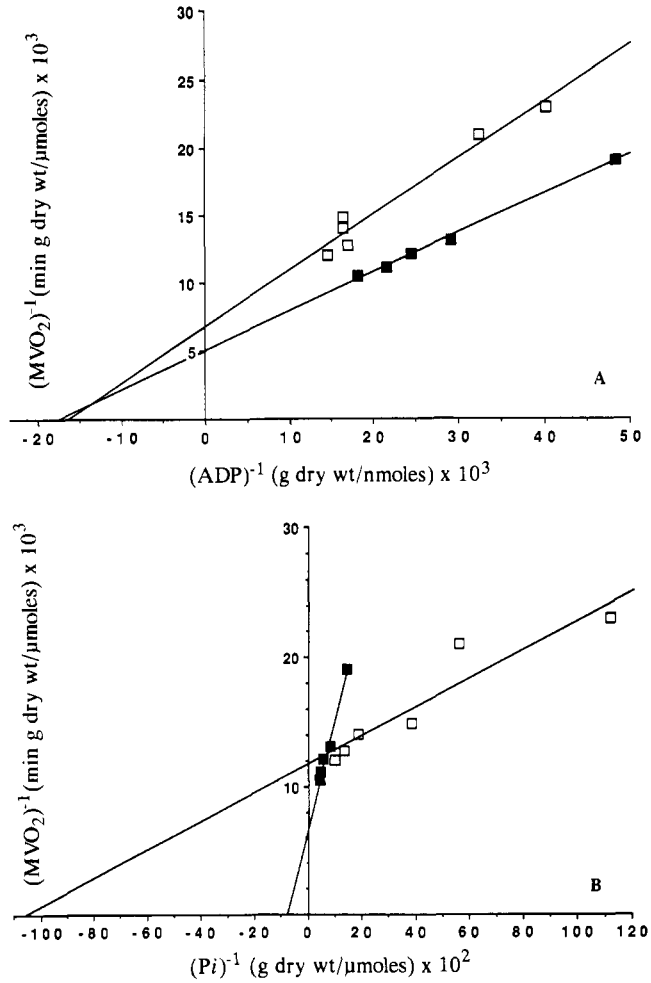

FIGURE 8: MVO_2^{-1} vs $[ADP]^{-1}$ (panel A) or $[P_i]^{-1}$ (panel B) in PG-perfused hearts under normal conditions (open squares) and following an ischemic episode (closed squares) which resulted in decreased ATP levels and elevated P_i levels but which did not induce any alteration in either postischemic mechanical function (RPP) or MVO_2 at any of the five workstates examined.

Kinetic Analyses—Two-Substrate Model

In principle, analysis of the dependence of MVO_2 upon the concentrations of its substrates (ADP, P_i, and NADH), within the context of Michaelis–Menten kinetics, should utilize a multisubstrate model. When NADH levels are high and virtually invariant, the analysis reduces to two-substrate Michaelis–Menten kinetics (see Materials and Methods for more details) described by

[3] When a multisubstrate kinetic scheme (e.g., eq 1) is reduced to a model where the reaction velocity is analyzed as a function of a single substrate, the K_m and V_{max} values extracted will be referred to as the *apparent* values. These will depend upon the concentrations of the other substrates involved in the reaction and may differ from the *limiting* K_m and *true* V_{max} values, which are independent of substrate concentration.

[4] V_{max} for MVO_2 was extrapolated from isolated rat heart mitochondrial state 3 respiration of 842 nanoatoms of O_2 (mg of mitochondrial protein)$^{-1}$ min^{-1} and an estimated 280 mg of mitochondrial protein gdw^{-1} of rat myocardium (La Noue et al., 1986). This calculation yields a V_{max} value of approximately 118 μmol min^{-1} gdw^{-1}. If one then considers that state 3 respiration of isolated mitochondria can be increased substantially by addition of physiologic quantities of Ca^{2+} which activate intramitochondrial dehydrogenases (Denton & McCormack, 1986a), then the extrapolated V_{max} for MVO_2 may be as high as 130–160 μmol min^{-1} gdw^{-1}.

$$V_{max}/MVO_2 = 1 + K_m^a/[ADP] + K_m^P/[P_i] + K_i^a K_m^P/[ADP][P_i] \quad (1)$$

In this equation, K_m^a and K_m^P are the limiting Michaelis–Menten constants for ADP and P_i, respectively, K_i^a is the inhibition constant for ADP, and V_{max} is the estimated maximal MVO_2. The oxygen consumption rate of isolated mitochondria examined in the presence of varying ADP and P_i concentrations, and presumably in the presence of nonlimiting NADH, was shown to fulfill this equation (Stoner & Sirak, 1979). In this model, a linear interdependence between MVO_2 and each of the two substrates (i.e., ADP or P_i) is possible under certain conditions [discussed in detail in Zimmer et al. (1989)].

When the PG data were fitted to eq 1 to extract the parameters K_m^a, K_m^P, and V_{max} by nonlinear optimization (Zimmer et al., 1989), the "best fit" (i.e., the minimum χ^2 fit) yielded $V_{max} = 120 \pm 3$ μmol min^{-1} gdw^{-1}, $K_m^a = 11.8 \pm 0.7$ μM, and $K_m^P = 0.43 \pm 0.06$ μM. Due to covariance, the ranges of acceptable fits were as follows: V_{max}, 120–170 μmol of O_2 min^{-1} gdw^{-1}; K_m^a, 10–26 μM; K_m^P, 0.2–0.65 mM. One such acceptable fit was $V_{max} = 159$ μmol of O_2 min^{-1} gdw^{-1} and $K_m^a = 25$ μM, values quite indistinguishable from those obtained from the same group by the single-substrate kinetic model (see above and Table VI).

When a similar fit was made for the aforementioned postischemic PG data, the best fit gave $V_{max} = 186 \pm 8$ μmol min^{-1} gdw^{-1}, $K_m^a = 20.6 \pm 1.6$ μM, and $K_m^P = 0.01 \pm 0.6$ mM, with a similar range of acceptable fits as in controls due to covariance. K_m^a is quite comparable to the corresponding apparent K_m value obtained from this group with the single-substrate kinetic model (see above).

Effects of Endogenous Lipid Consumption on Metabolic Regulation in Relation to Exogenous Substrates

To directly evaluate the role of endogenous lipid consumption, β-oxidation was blocked by addition of 13 μM 4-bromocrotonic acid to the perfusate (Hutter et al., 1984) of the PG, G, GI, and Lac groups. Neither mechanical function nor the regulatory pattern was altered in the PG group (data not shown). In the G group, mechanical activity was markedly limited when BCA was present (Table V); both RPP and MVO_2 peaked at the third workstate and then fell with increasing workstates. Beyond the third workstate, CP and ATP contents also fell, and ADP content continued to rise dramatically with increasing workstates despite decreasing MVO_2. It is clear that glucose without insulin is an inadequate carbon source when endogenous lipid consumption is not available to support higher levels of MVO_2.

In contrast, BCA had only modest effects upon the peak MVO_2 and RPP attained in the GI group (data not shown). This result demonstrates that, with glucose in the presence of insulin, endogenous lipid utilization is required to support ATP synthesis only at the highest MVO_2 values achieved in this study. In an earlier study (Kobayashi & Neely, 1979) performed with GI-perfused working hearts, ATP synthesis also became dependent upon endogenous fatty acid utilization at relatively high MVO_2 values.

In the Lac group of hearts (Tables III and V) BCA had no effects upon MVO_2 or RPP achieved. However, there was a marked influence of BCA upon ADP levels and MVO_2–ADP content relationship (Table V, Figure 7). This suggests that, even in the Lac group, endogenous lipid consumption contributed to ATP synthesis at high workstates as demonstrated by Kobayashi and Neely (1979). Had the Lac group achieved the higher MVO_2 values characteristic of the working heart, a dependence upon endogenous lipid consumption likely would have been more pronounced (Kobayashi & Neely, 1979).

Effects of Activation of Pyruvate Dehydrogenase by Dichloroacetic Acid

To evaluate the possibility that conversion of pyruvate to acetyl-CoA by the PDH complex (in addition to glucose transport into the cell and glycolytic reactions) was rate limiting in G and GI groups at low workloads, we evaluated the effects of 1 mM DCLA upon mechanical performance, MVO_2, and high-energy phosphate response in the presence of BCA. The use of BCA removed the effects of endogenous lipid consumption on the metabolic responses and permitted PDH to be evaluated as a potentially rate-limiting step for generation of intramitochondrial acetyl-CoA. In the G + BCA group (Table V), addition of DCLA caused a marked improvement in the maximal RPP and MVO_2 achieved and resulted in lower ADP levels at a given MVO_2 value; it should be noted, however, that maximal performance was still limited in this group. DCLA did not have significant effects in the GI group (data not shown).

Discussion

(I) Relationship of Current Observations to Previously Proposed Models of Respiratory Regulation

Near-Equilibrium Hypothesis. Previously proposed mechanisms for mitochondrial respiratory control are based upon the opposing concepts of either thermodynamic (i.e., near equilibrium) regulation or kinetic rate control under conditions that are far from equilibrium. The near-equilibrium hypothesis posits that the reactions in the electron-transport chain from NADH oxidation to reduction of Cyt *c* are in virtual equilibrium with each other and with the mitochondrial H^+-ATPase via the mitochondrial transmembrane proton electrochemical gradient [see Erecinska and Wilson (1982) for review]; in turn, the mitochondrial ATP, ADP, and P_i levels are postulated to be in equilibrium with their cytosolic counterparts through the activities of the appropriate systems. The cytochrome oxidase reaction is irreversible and rate limiting, and its rate is determined by the level of its substrate (i.e., reduced Cyt *c*). Within the context of this postulate, the product of [Cyt *c*(II)]/[Cyt *c*(III)], mitochondrial [NAD]/[NADH], and cytosolic $([ATP]/[ADP][P_i])^q$ is a constant, where *q* is usually taken to be 2 on the basis of the stoichiometries of proton extrusion and utilization by the electron-transport chain and the mitochondrial H^+-ATPase, respectively. Therefore, according to the near-equilibrium hypothesis, it is possible to alter the Cyt *c*(II) level by changing either the cytosolic PP or the mitochondrial NAD/NADH ratio of both and, by this means, regulate the rate of oxygen consumption. This is the rationale for PP being a regulatory parameter and the reason why all the numerous experimental observations documenting an inverse relation between PP and MVO_2 in intact cells and tissues as well as in isolated mitochondria have been interpreted as being supportive of the near-equilibrium concept. Further, according to the near-equilibrium hypothesis taken in its general form, PP is not required to be fixed with regard to a given value of MVO_2 but can vary depending on the level of NADH in the mitochondrial matrix (Erecinska & Wilson, 1982; Starnes et al., 1985). Therefore, in the absence of data on mitochondrial [NAD]/[NADH], the near-equilibrium hypothesis is not contradicted by either the recent isolated mitochondrial data (Jacobus et al., 1982) illustrating that the usual inverse relationship between QO_2 and PP can in fact be reversed to a direct relationship or previous (Starnes et al., 1985; Balaban et al., 1986; Robitaille et al., 1990; From et

al., 1986) and present data (Figure 4) which demonstrate that there is no unique value of PP associated with a given MVO_2 in the intact myocardium.

However, recent data on ATP synthesis and hydrolysis kinetics provide direct evidence against the fundamental assumption of the near-equilibrium hypothesis, namely, that mitochondrial H^+-ATPase must be near equilibrium. We have recently reported that, in the intact perfused heart, the unidirectional ATP $\rightarrow$ ADP + P_i rate (v_2) for the mitochondrial H^+-ATPase is negligible even at the lowest MVO_2 values examined (30 μmol of O_2 min^{-1} gdw^{-1}), while the unidirectional ADP + P_i $\rightarrow$ ATP rate (v_1) increases linearly with increasing MVO_2 (Kingsley-Hickman et al., 1987). Similarly, LaNoue et al. (1986) recently demonstrated that, in isolated rat liver and rat heart mitochondria, oxidative phosphorylation was not near equilibrium except at or near state 4 respiratory conditions. An *upper* limit for the state 4 respiratory state for intact myocardium is provided by MVO_2 determinations in K^+-arrested hearts; MVO_2 in such hearts can be as low as 6 μmol min^{-1} gdw^{-1} (Matthews et al., 1982). This is much lower than the range of MVO_2 values evaluated in both our kinetic studies (Kingsley-Hickman et al., 1987) and the current study. Therefore, the data of LaNoue et al. (1986) would also predict that $v_1 \gg v_2$ in the intact heart under the conditions of our kinetic studies (Kingsley-Hickman et al., 1987) and in the current studies.

Possible Kinetic Regulatory Mechanisms. Excluding the near-equilibrium or thermodynamic regulation as a viable mechanism for respiratory regulation requires that we must examine the second class of previously proposed regulatory mechanisms based upon kinetic regulation under nonequilibrium conditions.

(*i*) *ATP/ADP Ratio.* The cytosolic ATP/ADP ratio has been postulated to be the determinant of the rate of turnover of the adenine nucleotide translocase, which, in turn, has been suggested to be a rate-determining step in oxidative phosphorylation (Kunz et al., 1981; Tager et al., 1982). The "translocase" hypothesis requires that a unique value of the ATP/ADP ratio is associated with any given MVO_2. However, such a relationship is clearly absent in the data obtained on the isolated perfused heart (Figure 5). Additionally, the ATP/ADP ratio does not appear to vary with RPP under in vivo conditions (Balaban et al., 1986; Robitaille et al., 1990). These observations contradict regulatory claims for this parameter.

(*ii*) *ADP Availability.* Similarly, ADP availability (Chance & Williams, 1985) alone cannot universally determine the mitochondrial respiration rate in the myocardium. In the perfused heart, the ADP level at any given MVO_2 is determined by the exogenous carbon source (Tables II–V; Figures 5–7). Thus, the myocardium can attain the same MVO_2 at very different cytosolic ADP levels, some of which are far in excess of the apparent K_m measured for ADP from QO_2–[ADP] interdependence in isolated mitochondrial preparations (Chance & Williams, 1955; Stoner & Sirak, 1979; Jacobus et al., 1982). Further, in the in vivo canine heart, neither Balaban et al. (1986) nor we (Robitaille et al., 1990) found any change in estimated ADP levels over a large range of RPP.

While ADP limitation cannot be the universal determinant of respiratory regulation, with at least three carbon sources examined in this study it appears to be applicable. In the PG, Lac + BCA, and Oct-2 groups, cytosolic free ADP levels in the myocardium were very low (less than or comparable to the apparent ADP K_m). For these carbon groups, MVO_2^{-1} exhibited a linear dependence on $[ADP]^{-1}$ (Figures 5–7). This Michaelis–Menten relationship between MVO_2 and [ADP], either in the context of the two substrate model (eq 1) or in the further simplified single-substrate approximation, yields *limiting* or *apparent* K_m values, respectively, which are comparable to those observed in isolated mitochondria (Chance & Williams, 1955; Jacobus et al., 1982). Similarly, calculated V_{max} values are consistent with values extrapolated from isolated mitochondrial data.[4] It should be noted that apparent ADP K_m values obtained in mitochondrial suspensions cover a fairly large range and vary with assay conditions [e.g., Jacobus et al. (1982)].

(*iii*) P_i *Availability.* With respect to P_i, the data (Tables II–IV and VII; Figure 8) lead to a conclusion similar to that reached for ADP. Namely, while P_i alone cannot be the universal regulator of MVO_2, in PG- and possibly Palm-perfused hearts it is sufficiently low to approach rate-limiting levels at low workstates.

(II) Integrated Model of Kinetic Regulation of Respiration

A unifying and general mechanism of respiratory control which is consistent with all present in vivo and in vitro data is *kinetic rate control* through the availability of the primary substrates of oxidative phosphorylation, i.e., NADH, ADP, P_i, and O_2. The current study is restricted to conditions where O_2 is in excess; therefore, only the case of rate control through the levels of ADP, P_i, and NADH will be considered. This is essentially a problem of three-substrate kinetics where the relationship between a single substrate and the reaction rate will yield apparent K_m and V_{max} values that will depend on the concentrations of the other two substrates. In this scheme, it is not possible at present to provide a rigorous quantitative model for the interdependence of the concentrations of the three substrates and the reaction rate, especially when NADH levels are nonsaturating and vary with MVO_2. Such a model would require detailed kinetic information, including regulatory influences of the various compounds on all enzymes involved. However, the behavior of the reaction rate (i.e., MVO_2) under limiting conditions can be predicted. There exist two specific limiting conditions that are of particular interest. The first is the state achieved when NADH is in excess but the ADP and/or P_i level is sufficiently low to be rate limiting, and the second is the converse situation where NADH, rather than ADP and P_i, is rate limiting.

ADP- and P_i-Limited Domain. Within the concept of the proposed kinetic model, MVO_2 should be dependent on ADP and/or P_i levels provided that NADH levels do not change significantly with MVO_2 or that NADH remains high relative to its limiting K_m and inhibition constants. In its least complex form, this interdependence will be through simple two-substrate Michaelis–Menten kinetics (eq 1), which can, under certain circumstances, lead to a linear relationship between inverse MVO_2 and inverse [ADP] or [P_i]. If the model is sufficiently valid, then the limiting K_m values obtained for ADP and P_i in intact myocardium should be similar to values measured in isolated mitochondria with rate-determining ADP and/or P_i levels but with abundant O_2 and exogenous carbon source.

In the intact myocardium, the ADP- and P_i-limited domain is exemplified by the PG- and Oct-2-perfused hearts where ADP and P_i levels are low and change with MVO_2, and analysis of data, either according to eq 1 or according to the further simplified single-substrate approximation, yields ADP and/or P_i K_m values in agreement with values derived from mitochondrial studies. There is evidence (to be discussed subsequently) that a major result of both pyruvate or octanoate perfusion is to increase the levels of acetyl-CoA and TCA cycle

intermediates and, in consequence, to deregulate mitochondrial NADH production. Under these circumstances, NADH availability to the electron-transport chain should be nonlimiting to the rate of oxidative phosphorylation. Within the kinetic regulatory concept under consideration, the presence of excess (nonlimiting) levels of mitochondrial NADH should generate the condition where the rate of ATP synthesis would be ultimately limited by [ADP] and/or [P_i].

To further test this concept, we altered the relationship between ADP and P_i levels by using a transient ischemic period which did not have any detrimental mechanical consequences. As a result, postischemic P_i levels were dramatically elevated while the total adenine nucleotide pool was reduced. Within the concept of kinetic regulation through availability of substrates P_i, ADP, NADH, and O_2, this selective increase in the P_i levels should influence the MVO_2–[ADP] relationship as well as the MVO_2–[P_i] relationship. This is indeed the case (Figure 8). The apparent K_m for ADP (obtained from the [ADP]–MVO_2 interdependence alone without considering the P_i levels) is now lower, and the MVO_2^{-1}–$[ADP]^{-1}$ plot is shifted. Similarly, the MVO_2^{-1}–$[P_i]^{-1}$ relationship is altered. On the other hand, fitting the postischemic data to the simple two-substrate Michaelis–Menten model (eq 1) yields parameters that overlap those obtained from the nonischemic PG group. Again, due to the complexity of the problem, it is difficult to analyze the data quantitatively with greater rigor. However, the changes in the [single-substrate]–MVO_2 relationship and the analysis according to the two-substrate kinetic model are qualitatively consistent with the kinetic regulatory scheme proposed.

NADH-Limited Domain. In this domain, ADP and P_i levels are high and not rate limiting, but NADH levels are low and rate limiting. This is approximately the case of the glucose-perfused heart where ADP and P_i levels are indeed high and the ADP level changes very little with increasing MVO_2. However, the NADH levels are much lower in glucose-perfused hearts than those obtained in pyruvate-perfused hearts and increase with increasing MVO_2 (Katz et al., 1986). Similar observations with regard to NADH have been made in isolated rabbit papillary muscles (Chapman et al., 1976). Quantitative data on [NADH]–MVO_2 interdependence similar to the MVO_2–[ADP] relationship shown in Figure 5, however, do not exist for perfused heart preparations.

(III) Relationship between Carbon Source and Coupling of ATP Consumption to Oxidative Phosphorylation

The discussion, thus far, has focused upon ADP, P_i, and NADH as determinants of MVO_2. However, three additional and related questions that are relevant to mitochondrial function in the intact cell must also be considered: (i) At a constant MVO_2, what sets the levels of NADH, ADP, and P_i for the different exogenous carbon substrates? (ii) By which mechanisms are increases in MVO_2 and [NADH] achieved with increasing mechanical output in states where the ADP level changes relatively little with MVO_2 (i.e., in G, GI, Palm-, and Lac-perfused hearts and the heart in vivo)? (iii) What is the mechanism of coupling between the ATP consumption rate (determined primarily by mechanical activity of the heart) and the oxygen consumption rate?

(i) NADH, ADP, and P_i Levels vs Carbon Source. The first question arises from evidence that both in situ mitochondria (Starnes et al., 1985; From et al., 1986; current data) and isolated mitochondria (Koretsky et al., 1987) can attain the same O_2 consumption rate at very different levels of NADH, ADP, and P_i. The concept of kinetic regulation of MVO_2 through NADH, ADP, and P_i levels already outlined accommodates this observation. This follows simply from the fact that, in a multisubstrate reaction, the same reaction rate can be achieved by different combinations of the levels of the various reactants. However, this concept, by itself, does not deal with the question of why myocardial NADH, ADP, and P_i levels differ at the same MVO_2 value when the exogenous carbon source is altered. The explanation of this phenomenon involves the kinetic properties of the TCA cycle enzymes responsible for mitochondrial NADH generation. There are two major points that should be noted: First, the activities of PDH and the dehydrogenases involved in the TCA cycle are known to be influenced by Ca^{2+}, NAD/NADH, ATP/ADP, and substrates such as pyruvate and acetyl-CoA in the specific case of PDH (Bremer, 1969; Hansford & Johnson, 1975; McCormack & Denton, 1979, 1986a,b; Rutter & Denton, 1988). Second, as is well-known, the rate of an enzyme-catalyzed reaction depends on the concentration of substrates as well as products even in the absence of regulatory influences. Therefore, the level of TCA cycle substrates, intermediates, and products must be considered. Both of these points are important in the context that when the rate of NADH synthesis is fixed at a given MVO_2, the position of the rate-determining steps within or prior to the TCA cycle will influence the overall level of TCA cycle intermediates and the level of NADH at that particular turnover rate. For simplicity, let us consider the extreme cases first. If the primary rate-determining step in TCA cycle turnover and in oxidative phosphorylation is acetyl-CoA generation, then the levels of acetyl-CoA and NADH (which is produced "downstream" of the acetyl-CoA formation step) should be low. Of course, by postulating the rate-determining step to be acetyl-CoA generation, we assume that the downstream enzymes have the capacity to operate at much higher rates but do not simply because of the limitation imposed by the rate of acetyl-CoA formation. If, on the other hand, acetyl-CoA formation or any other subsequent TCA cycle step is not rate determining and the TCA cycle turnover rate is determined only by the clearance of the TCA cycle end product, NADH, then the level of NADH should be high. In the latter case, the level of TCA cycle intermediates will also be high in the presence of sufficient anaplerosis. In other words, the concentrations of the substrates upstream of the rate-determining step will be elevated.

The comparisons of G + BCA vs G + BCA + DCLA, G ± I vs PG, and Oct vs Palm data support the validity of the concept that the position of the rate-determining step in the mitochondrial NADH synthesis pathway is the primary factor affecting the levels of NADH and ultimately ADP and P_i levels. When 10 mM pyruvate (PG group) is the carbon source, PDH is highly activated, and the mitochondrial acetyl-CoA content and the level of NADH and other TCA cycle intermediates (via anaplerotic mechanisms) are high (Chapman, 1972, 1976; Katz et al., 1986, 1987; Kobayashi & Neely, 1979; Peuhkurinen, 1984). On the other hand, with glucose hearts, intracellular pyruvate concentrations are very low (Williamson, 1965) and most probably below the levels needed to maximally activate PDH (Dennis et al., 1979). Therefore, the PDH reaction, and ultimately other reactions responsible for pyruvate generation and anaplerosis, may become the primary "upstream" rate-limiting steps that control TCA cycle turnover. If PDH is imposing a rate limitation beyond that of the ability of the glycolytic pathway to supply pyruvate, then activating PDH in glucose-perfused hearts should lead to higher NADH and consequently lower ADP levels at a given MVO_2 but should not induce the levels observed in pyru-

vate-perfused hearts because of the ultimate limit upon the rate of pyruvate generation and anaplerosis imposed by glycolysis. This is indeed observed when DCLA is added to the perfusate of G hearts with fatty acid oxidation blocked by BCA (Table V).

Similarly, previous studies of perfused rat hearts have shown that the rate-determining step in long-chain fatty acid utilization is the long-chain acylcarnitine transferase step and that acetyl-CoA levels are not saturating at high workstates when long-chain fatty acids are the carbon source (Neely et al., 1972). Therefore, in Palm-perfused hearts (and most probably in vivo) even though ADP levels are low and acetyl-CoA and presumably NADH levels are high, they are not high enough to be saturating. Bypassing the acylcarnitine transferase step with octanoate, an intervention that maintains high levels of acetyl-CoA even at high workstates (Neely et al., 1972) and is associated with elevated TCA cycle intermediate levels (Sundquist et al., 1984), shifts the system to lower ADP levels (Table IV and Figure 6) and to higher NADH levels (Pearce et al., 1979). As a result, ADP levels fall into the regulatory range (Figure 6).

The question of the rate-determining step can become a complex issue with some substrates or mixtures of substrates. G and Lac groups are two such cases. With glucose as the exogenous carbon source, ADP levels first increase and then decrease with increasing MVO_2. The decrease at high MVO_2 values is temporally associated with the onset of endogenous lipid utilization as illustrated with experiments using BCA. With lactate as the carbon source, ADP levels are not much higher than those found in the pyruvate group. They increase with increasing MVO_2 initially and subsequently stabilize. In the Lac + BCA group, however, ADP continues to increase with increasing MVO_2 (Figure 7; Table V). Hence, it is likely that NADH levels in the Lac group, although higher than those found in the glucose groups (Chapman, 1972), are still subject to work-related augmentation by endogenous lipid utilization.

It is important to emphasize that we are not proposing the exogenous carbon source to be the regulator of the *rate* of oxidative phosphorylation. Rather, we suggest that the type of carbon source influences the levels of the primary substrates of respiration (i.e., ADP, P_i, and NADH in the presence of nonlimiting O_2) such that the *regulatory domain* rather than the *rate* of respiration is affected. Hence, the same level of MVO_2 can be associated with differing levels of ADP, P_i, and NADH. This concept differs somewhat from that presented by Brand and Murphy (1987), based upon studies of liver, wherein changing the exogenous carbon source may affect the *rate* of respiration.

(ii) NADH Levels vs MVO_2 When ADP and/or P_i Levels Are High. With exogenous carbon sources that are associated with relatively high levels of ADP and/or P_i (i.e., glucose or submaximal pyruvate concentrations), there is evidence in both perfused heart and isolated papillary muscle preparations that NADH fluorescence increases in concert with increasing MVO_2 or mechanical output (Katz et al., 1986, 1987; Chapman et al., 1976). Presumably, similar events may occur under in vivo conditions, considering the apparent stability of cytosolic ADP levels in relation to increasing ATP consumption (Balaban et al., 1986; Robitaille et al., 1990). One explanation for the increase of NADH with workload is Ca^{2+} activation of the TCA cycle dehydrogenases. As is well-known, two of the major physiologic mechanisms for increasing cardiac work (increasing heart rate and catecholamine inotropism) are associated with increased frequency and/or amplitude of the cytosolic Ca^{2+} transient (Morgan & Blinks, 1982); this results in elevation of "time-averaged" cytosolic Ca^{2+} levels. It is also well-known that respiring mitochondria actively take up Ca^{2+} from the extramitochondrial milleau in relation to extramitochondrial [Ca^{2+}] (Nicholls & Ackerman, 1982). Thus, as "average" cytosolic Ca^{2+} levels rise with increasing MVO_2 in the present work (where workstate increments were primarily the result of increased heart rate and catecholamine stimulation), it might be expected that mitochondrial matrix Ca^{2+} would rise and that the salient dehydrogenases would be activated as suggested by Denton and McCormack (1986a,b). It must also be noted that under these conditions all possible rate-limiting steps upstream of the TCA cycle dehydrogenases must also be somehow activated or regulated. These include rate-limiting steps in glycolysis when glucose is the primary exogenous carbon source or fatty acid activation, acylcarnitine transferase, and lipid β-oxidation when long-chain fatty acids are the exogenous carbon source.

The dehydrogenase activation mechanism, however, is most probably much more complex than the aforementioned Ca^{2+} regulatory hypothesis would imply. For example, we (Lew et al., 1988) have found that ruthenium red, an agent previously shown to block Ca^{2+}-induced activation of PDH in perfused rat hearts (McCormack & England, 1983; McCormack & Denton, 1986b; Unitt et al., 1989) and in isolated myocytes (Hansford, 1987; Moreno-Sanchez & Hansford, 1988), only modestly affects either maximal MVO_2 attainable in perfused rat hearts or the calculated cytosolic [ADP] over a wide range of workstates. Similarly, Katz et al. (1988) have shown that ruthenium red does not block the pacing-induced elevation of MVO_2 in perfused rat hearts. Last, Crompton and Goldstone (1986) have shown that the sustained stimulation of hepatocyte respiration induced by isoproterenol was not correlated with changes in cytosolic Ca^{2+}, and Lakin-Thomas and Brand (1988) have shown that mitogenic stimulation of respiration in thymocytes was independent of the size of the mitochondrial Ca^{2+} pool. While these observations do not preclude the effects of changes in cytosolic and/or mitochondrial matrix Ca^{2+} levels upon dehydrogenase activity being of great physiologic importance, they do indicate that other activating mechanisms are present and quite effective in expediting TCA cycle flux when work-related increases of mitochondrial Ca^{2+} influx are blocked. The observations of Lew et al. (1988) also do not preclude the possibility that altered workstate may increase mitochondrial matrix [Ca^{2+}] by mobilizing bound intramitochondrial Ca^{2+} as suggested by Reers et al. (1989). Further, Halestrap (1989) has suggested that non-Ca^{2+}- as well as Ca^{2+}-mediated changes in mitochondrial matrix volume may stimulate respiration by activation of both lipid oxidation and the respiratory chain itself; it is possible that such changes occur with increasing workstate.

(iii) Mechanical Work–MVO_2 Coupling. Mechanical work and MVO_2 are tightly coupled in the myocardium. This coupling must be mediated through a feedback loop. The obvious candidates to mediate such a feedback coupling are ADP and P_i since they are the products of one process and the substrate for the other. This type of coupling can be accommodated within the concept of kinetic respiratory control through rate regulation by the substrates NADH, ADP, and P_i. In this concept, or actually in any multiple-substrate enzyme kinetics problem, each substrate influences the overall rate. In the specific case of the three-substrate kinetics involving NADH, ADP, and P_i, two different MVO_2 values can be achieved at the same ADP and P_i levels when the NADH is altered by an appropriate amount. Another way of visu-

alizing this problem is that while ADP and P_i levels remain constant, the *apparent* K_m and/or V_{max} values for these substrates in the MVO_2–[substrate] relationship are altered due to changes in the concentration of the third substrate. The two descriptions are equivalent. Therefore, the kinetic rate regulation through the levels of NADH, ADP, and P_i can provide ADP- and P_i-mediated coupling between respiration and mechanical work even when ADP and P_i levels remain constant with increasing MVO_2, as is the case in the in vivo heart.

By affecting both the activities of the force-generating processes and the TCA cycle dehydrogenases, Ca^{2+} most probably influences the coupling between these two types of processes, although, as pointed out above, work-related changes of mitochondrial Ca^{2+} influx cannot be the sole mediator of dehydrogenase activation. Further, the concept of fine control of two different sets of processes exclusively through the level of a third agent is an extremely difficult one because a steady state cannot be achieved if the rates for each set of processes are not set exactly equal by the third agent (i.e., Ca^{2+}). Thus, while Ca^{2+} and other mediators that influence dehydrogenase activation probably play an important role in this process, the fine adjustment of the rate of oxidative phosphorylation likely comes through a feedback loop that involves the cytosolic ADP and P_i levels.

The general conclusions reached in this study about the regulation of oxidative phosphorylation rate are likely to be applicable to all cell types that are primarily oxidative in their metabolism. This view is supported by the finding that in vitro regulatory characteristics and kinetics of liver and myocardial mitochondria are similar [see, for example, LaNoue et al. (1986)]. However, the operative regulatory domain defined by the relative concentrations of NADH, ADP, P_i, and O_2 may differ for each cell type and most likely depends upon the other functional requirements of the cell.

ACKNOWLEDGMENTS

The technical assistance of Michael Barone and the assistance of Kathy Stattine in preparing the manuscript are gratefully acknowledged.

Registry No. P_i, 14265-44-2; 5′-ATP, 56-65-5; 5′-ADP, 58-64-0; NADH, 58-68-4; glucose, 50-99-7; insulin, 9004-10-8; palmitic acid, 57-10-3; lactic acid, 50-21-5; pyruvic acid, 127-17-3; octanoic acid, 124-07-2; creatine phosphate, 67-07-2; pyruvate dehydrogenase, 9014-20-4.

REFERENCES

Allen, D. G., & Kentish, J. C. (1985) *J. Mol. Cell. Cardiol. 17*, 821–840.

Al Makdessi, S., Andrieu, J. L., Herilier, H., & Faucon, G. (1987) *J. Mol. Cell. Cardiol. 19*, 141–149.

Bailey, I. A., Williams, S. R., Radda, G. K., & Gadian, D. C. (1981) *Biochem. J. 196*, 171–178.

Balaban, R. S., Kantor, H. L., Katz, L. A., & Briggs, R. W. (1986) *Science 232*, 1121–1123.

Bittl, J. A., & Ingwall, J. S. (1985) *J. Biol. Chem. 260*, 3512–3517.

Bradshaw, R. A., Robinson, G. W., Hass, G. M., & Hill, R. L. (1969) *J. Biol. Chem. 244*, 1755–1763.

Brand, M. D., & Murphy, M. P. (1987) *Biol. Rev. 62*, 141–193.

Bremer, J. (1969) *Eur. J. Biochem. 8*, 535–540.

Chance, B., & Williams, G. R. (1955) *J. Biol. Chem. 217*, 383–393.

Chapman, J. B. (1972) *J. Gen. Physiol. 59*, 135–154.

Chapman, J. B., Gibbs, C. L., & Gibson, W. R. (1976) *J. Mol. Cell. Cardiol. 8*, 545–558.

Crompton, M., & Goldstone, T. P. (1986) *FEBS Lett. 204*, 198–202.

Dennis, S. C., Padma, A., DeBuysere, M. S., & Olson, M. S. (1979) *J. Biol. Chem. 254*, 1252–1258.

Erecinska, M., & Wilson, D. F. (1978) *Trends Biochem. Sci. 3*, 219–222.

Erecinska, M., & Wilson, D. F. (1982) *Membr. Biol. 70*, 1–14.

Erecinska, M., Stubbs, M., Miyata, Y., Ditre, C. M., & Wilson, D. F. (1977) *Biochim. Biophys. Acta 462*, 20–35.

From, A. H. L., Petein, M. A., Michurski, S. P., Zimmer, S. D., & Ugurbil, K. (1986) *FEBS Lett. 206*, 57–261.

Halestrap, A. P. (1989) *Biochim. Biophys. Acta 973*, 355–382.

Hansford, R. G. (1987) *Biochem. J. 241*, 145–151.

Hansford, R. G., & Johnson, R. N. (1975) *J. Biol. Chem. 250*, 8361–8375.

Hutter, J. F., Schweikhardt, C., Piper, H. M., & Spieckermann, P. G. (1984) *J. Mol. Cell. Cardiol. 16*, 105–108.

Jacobus, W. E., Moreadith, R. W., & Vandegaer, K. M. (1982) *J. Biol. Chem. 257*, 2397–2402.

Kammermeier, H., Schmidt, P., & Jungling, E. (1982) *J. Mol. Cell. Cardiol. 14*, 267–277.

Katz, L. A., Koretsky, A. P., & Balaban, R. S. (1986) *Circulation 74* (Suppl. II), II327 (Abstract).

Katz, L. A., Koretsky, A. P., & Balaban, R. S. (1987) *FEBS Lett. 221*, 270–276.

Katz, L. A., Koretsky, A. P., & Balaban, R. S. (1988) *Am. J. Physiol. 255*, H185–H188.

Kentish, J. C., terKeurs, H. E. D., Ricciardi, L., Bucx, J. J. J., & Noble, M. I. M. (1986) *Circ. Res. 58*, 755–768.

Kingsley-Hickman, P. B., Sako, E. Y., Mohanakrishnan, P., Robitaille, P.-M. L., From, A. H. L., Foker, J. E., & Ugurbil, K. (1987) *Biochemistry 26*, 7501–7510.

Kobayashi, K., & Neely, J. R. (1979) *Circ. Res. 44*, 166–175.

Kobayashi, K., & Neely, J. R. (1983) *J. Mol. Cell. Cardiol. 15*, 369–382.

Koretsky, A. P., & Balaban, R. S. (1987) *Biochim. Biophys. Acta 893*, 398–408.

Kunz, W., Bohnensack, R., Bohme, G., Kuster, U., Letko, G., & Schonfeld, P. (1981) *Arch. Biochem. Biophys. 209*, 219–229.

Lakin-Thomas, P. L., & Brand, M. D. (1988) *Biochem. J. 256*, 167–173.

La Noue, K. F., Jeffries, F. M. H., & Radda, G. K. (1986) *Biochemistry 25*, 7667–7675.

Lawson, J. W. R., & Veech, R. L. (1979) *J. Biol. Chem. 254*, 6528–6537.

Lew, B. T., Mohanakrishnan, P., Ugurbil, K., & From, A. H. L. (1988) *Soc. Magn. Reson. Med. Abstr. 7*, 290.

Matthews, P. M., Bland, J. L., Gadian, D. G., & Radda, G. K. (1982) *Biochim. Biophys. Acta 721*, 312–320.

McCormack, J. G., & Denton, R. M. (1979) *Biochem. J. 180*, 533–544.

McCormack, J. G., & England, P. J. (1983) *Biochem. J. 214*, 581–585.

McCormack, J. G., & Denton, R. M. (1986a) *Trends Biochem. Sci. 11*, 258–262.

McCormack, J. G., & Denton, R. M. (1986b) in *The Regulation of Heart Function* (Rupp, H., Ed.) pp. 186–200, Thieme, New York.

Mjos, O. D. (1971) *J. Clin. Invest. 50*, 1386–1389.

Moreno-Sanchez, R., & Hansford, R. G. (1988) *Am. J. Physiol. 255*, H347–H357.

Morgan, H. E., Regen, D. M., & Park, C. R. (1964) *J. Biol. Chem. 239*, 369–374.

Morgan, J. P., & Blinks, J. R. (1982) *Can. J. Physiol. Pharmacol. 60*, 524–530.
Neely, J. R., Rovetto, M. J., & Oram, J. F. (1972) *Prog. Cardiovasc. Dis. 15*, 289–329.
Nicholls, D. G., & Ackerman, K. E. O. (1982) *Biochim. Biophys. Acta 683*, 57–88.
Pearce, F. J., Forster, J., DeLeeuw, G., Williamson, J. R., & Tutwiler, G. F. (1979) *J. Mol. Cell. Cardiol. 11*, 893–915.
Peuhkurinen, K. J. (1984) *J. Mol. Cell. Cardiol. 16*, 487–495.
Reers, M., Kelly, R. A., & Smith, T. W. (1989) *Biophys. J. 55*, 32a (Abstract).
Robitaille, P.-M., Lew, B., Merkle, H., Path, G., From, A. H. L., Bache, R., & Ugurbil, K. (1990) *Magn. Reson. Med.* (in press).
Rutter, G. A., & Denton, R. M. (1988) *Biochem. J. 252*, 181–189.
Starnes, J. W., Wilson, D. F., & Erecinska, M. (1985) *Am. J. Physiol. 249*, H799–H806.
Stoner, C. D., & Sirak, H. D. (1979) *J. Bioenerg. Biomembr. 11*, 113–145.
Sundqvist, K. E., Peuhkurinen, K. J., Hiltunen, J. K., & Hassinen, I. E. (1984) *Biochim. Biophys. Acta 801*, 429–436.
Tager, J. M., Wanders, R. J. A., Groen, A. K., Kunz, W., Bohnensack, R., Kuster, U., Letko, G., Bohme, G., Duszynski, J., & Wojtczak, L. (1983) *FEBS Lett. 151*, 271–280.
Ugurbil, K., Petein, M., Maidan, R., Michurski, S., & From, A. H. L. (1986) *Biochemistry 25*, 100–107.
Unitt, J. F., McCormack, J. G., Reid, D., MacLachlan, L. K., & England, P. J. (1989) *Biochem. J. 262*, 293–301.
Vary, T. C., Reibel, D. K., & Neely, J. R. (1981) *Annu. Rev. Physiol. 43*, 419–429.
Williamson, J. R. (1965) *J. Biol. Chem. 240*, 2308–2321.
Williamson, J. R. (1966) *J. Biol. Chem. 241*, 5026–5036.
Zimmer, S. D., From, A. H. L., Foker, J. E., Michurski, S. P., & Ugurbil, K. (1987) *Ann. N.Y. Acad. Sci. 508*, 501–503.
Zimmer, S. D., Ugurbil, K., Michurski, S. P., Mohanakrishnan, P., Ulstad, V. K., Foker, J. E., & From, A. H. L. (1989) *J. Biol. Chem. 264*, 12402–12411.

Structure of the Rabbit Cytochrome P450IIC3 Gene, a Constitutive Member of the P450IIC Subfamily[†,‡]

Ging Chan[§] and Byron Kemper*
Department of Physiology and Biophysics, University of Illinois at Urbana–Champaign, Urbana, Illinois 61801
Received September 29, 1989; Revised Manuscript Received December 19, 1989

ABSTRACT: Fragments of rabbit DNA have been cloned which encompass the gene for rabbit cytochrome P450IIC3. Cytochrome P450IIC3 is a constitutive member of the cytochrome P450IIC subfamily which contains both constitutive and phenobarbital-responsive genes. The cytochrome P450IIC3 gene spans at least 25 kbp and contains 8 introns which have 5′ GT's and 3′ AG's and are located in the same positions as in other family II genes. The 5′ flanking region contains a consensus TATA site about 25 bp from the RNA initiation site which was mapped by the primer extension method. Other potential regulatory sequences include a CCAAT sequence and sequences similar to binding sites for the liver-specific factor HNF-1 and the general transcription factors AP-1 and OCT. The gene sequence differs from the cytochrome P450IIC3 cloned cDNA sequence in only 2 of 1400 nucleotides, 1 of which results in an amino acid change. Since sequences coding for exon 1 and part of exon 2 were not present in the cloned cytochrome P450IIC3 cDNA, a 475-nucleotide fragment of the 5′ end of the cDNA was amplified by the polymerase chain reaction, cloned, and sequenced. The sequence of this cDNA was identical with the gene exon sequence. The protein sequence derived from the gene differs in nine positions from that determined directly for the protein. A comparison of the amino acid sequence by exons with other cytochrome P450IIC proteins revealed that, in general, the similarity was greater in C-terminal exons than in N-terminal ones. This trend is exaggerated in the comparison with P450IIC4/5, for which exon 8 had a high similarity of 87% compared to 65% overall and 58% for exon 6. However, divergence of nucleotides that do not result in amino acid changes was similar in exon 5 and exon 8, indicating that gene conversion was not responsible for the difference in similarity between these two exons and suggesting that conservation of protein sequence in this region may be important.

Cytochrome P450IIC3 is a constitutive form of cytochrome P450 (P450)[1] in the rabbit liver that is not detectably induced by phenobarbital (Johnson, 1980; Koop & Coon, 1979) and metabolizes a variety of substrates, including polycyclic hydrocarbons, alcohols, macrolide antibiotics, and steroids. The enzyme is present in two catalytic forms in liver, one of which efficiently catalyzes both 6β- and 16α-hydroxylation of progesterone while the other is less efficient and catalyzes only 16α-hydroxylation of progesterone (Dieter & Johnson, 1982). The low-activity form is observed in some outbred animals and in some inbred strains, notably IIIVO/J and B/J. The low 16α-hydroxylase activity is stimulated by 5β-pregnane-

[†] This work was supported by grants from the Air Force Office of Scientific Research (AFOSR-84-103) and by the National Institutes of Health (GM 39360).
[‡] The nucleic acid sequence in this paper has been submitted to GenBank under Accession Number J02901.
* Correspondence should be addressed to this author at the Department of Physiology and Biophysics, 524 Burrill Hall, 407 S. Goodwin Ave., Urbana, IL 61801.
[§] Present address: Lilly Research Labs, Department of Molecular Biology, Building 98C/3, Indianapolis, IN 46285.

[1] Abbreviations: P450, cytochrome P450; kbp, kilobase pair(s).

0006-2960/90/0429-3743$02.50/0